Supplementary Material

Supplementary Methods

Table S1. Primers used for cloning and site-directed mutagenesis

Clone	Forward primer (5'-3')	Reverse primer (5'-3')
Sema6B, full cDNA	ATGTGGCCCCCCCTCGTC	CTATTTGCCCGAGGGAGTC
Sema6D, full cDNA	ATGAGGCTTCCTCTGCTGTG	CTAGTAACTGTATTTGTTCAGTGGTC TGA
Sema6B ΔmiR	GGAAGCTCACATGGCGATCCAATCA GCACGACATCAGCATC	CACGTGCTGATTGGATCGCCATGTGA GCTTCCGGTGATAGCG
PlexinA2 ΔmiR	GGAAGCTGTTCATAGGGACCGCTGTG GATGGGAAGC	CCACAGCGGTCCCTATGAACAGCT TCCCATCCTCG

To clone Sema6B into the pCAGGs vector, we added XbaI and BglII restriction sites to the forward and reverse primer, respectively. In addition, the forward primer contained the Kozak sequence (5'-GCCACCATGG) and the reverse primer was modified with an in-frame HA-tag sequence. The full-length Sema6BΔmiR and truncated Sema6BΔmiR version (lacking the intracellular sequence but maintaining the transmembrane domain and the first five intracellular amino acids) were inserted into the pMES-IRES-EGFP vector using XbaI and BglII restriction sites for the insert, and XbaI and BamHI for the vector. With the same restrictions sites we cloned the myc/his-tagged Sema6B constructs into pcDNA3.1 for *in vitro* assays. Similarly, full-length chicken PlexinA2ΔmiR and truncated PlexinA2ΔCTΔmiR (aa 1-1259) were cloned into pMath1-IRES-EGFP for specific expression in dI1 neurons (Wilson and Stoeckli, 2011).

Table S2. Target sequences of artificial miRNAs used in this study

Gene	Target sequence (5'-3')	Comment/Reference
Sema6B	AAGCTGACTTGGAGGTCGAACC	
PlexinA2	AAGCTCTTCATTGGCACGGCA	
Firefly Luciferase	CGTGGATTACGTCGCCAGTCAA	Wilson and Stoeckli, 2011

Table S3. ChESTs and cDNAs used to generate *in situ* hybridization probes and/or dsRNA

Gene	ChEST	Comment/Reference
Semaphorin6B	cDNA fragment	Mauti et al., 2006 and 2007
Semaphorin6D	225N10	ChEST
PlexinA1	53D13, 666O16	ChESTs
PlexinA2	128L21, 297D11	ChESTs
PlexinA4	1014M19, 202O14	ChESTs
Sonic hedgehog (Shh)	cDNA fragment	Bourikas et al., 2005
Slit2	cDNA fragment	Philipp et al., 2012

Chicken ESTs were purchased from Source BioScience LifeSciences, Nottingham, UK.

Table S4. Antibodies used in this study

Primary antibodies		
Protein detected	**Antibody**	**Company/Source**
myc-tagged Sema6B	mouse anti-Myc (9E10; hybridoma supernatant)	Developmental Studies Hybridoma Bank, Iowa City, IA, USA
HA-tagged PlexinA2	rabbit anti-HA (1:2,000)	Rockland Immunochemicals #600-401-384 Gilbertsville, PA, USA
Axonin1/Contactin2	rabbit anti-Axonin1 (1:1000)	Stoeckli and Landmesser, 1995
PlexinA1	rabbit anti-PlexinA1 (1:200)	Atlas Antibodies, #HPA007499, Stockholm, Sweden
PlexinA2	goat anti-PlexinA2 (1:200)	R&D Systems, #AF5486 Abingdon, UK
PlexinA4	rabbit anti-PlexinA4 (1:200)	Abcam, #ab39350 Cambridge, UK
Sema6B	goat anti-Sema6B (1:20)	R&D Systems, #AF2094
EBFP2	Fluorescein-conjugated goat anti-GFP (1:500)	Rockland Immunochemicals, #600-102-215
Hnf3β	mouse anti-Hnf3β (4C7; hybridoma supernatant)	DSHB
Nkx2.2	mouse anti-Nkx2.2 (74.5A5; conc. supernatant)	DSHB
Neurofilament	mouse anti-Neurofilament (4H6; supernatant)	DSHB
Fc-tagged Sema6 (Western blot)	Alexa-488 goat anti-human IgG (1:10,000)	Invitrogen, #A11013 Paisley, UK
Secondary antibodies		
Mouse IgG	donkey anti-mouse IgG-Cy3 (1:250)	Jackson ImmunoResearch, #715-165-150 West Grove, PA, USA
Mouse IgG	goat anti-mouse IgG-Alexa488 (1:250)	Invitrogen, #A11001
Rabbit IgG	donkey anti-rabbit IgG-Cy3 (1:250)	Jackson ImmunoResearch, #711-165-152
Goat IgG	donkey anti-goat IgG-Cy3 (1:250)	Jackson ImmunoResearch #705-165-147

Mouse IgG (Western blot)	sheep anti-mouse peroxidase (1:10,000)	Sigma-Aldrich, #A6782 St.Louis, MO, USA
Goat IgG (Western blot)	rabbit anti-goat peroxidase (1:10,000)	MP Biomedicals, #55358 Santa Ana, CA, USA

Table S5. Concentrations and *in vivo* electroporation parameters used in this study

Experiment/Figure	Concentration	Electroporation Parameters
Fig.1; Fig. 3; Fig. 6 (Long dsRNA)	300 ng/µl dsRNA 20 ng/µl EGFP plasmid	Unilateral, dorsal or ventral targeting (manual positioning) 5 x 50 ms pulses; 25 V
Fig. 2; Fig. S1 (miS6B, rescue constructs)	300 ng/µl miRNA construct 500 ng/µl rescue construct	Unilateral or dorsal targeting (manual positioning) 5 x 50 ms pulses; 25 V
Fig. 4 (miPA2, rescue constructs)	1 µg/µl miRNA construct 1 µg/µl rescue construct	Floorplate-specific targeting (*Hoxa-1* enhancer-driven) Bilateral; for each side: 5 x 50 ms pulses; 18V
Fig. 5, Fig. S2K (miS6B, miLuc)	300 ng/µl miRNA construct	Unilateral targeting 5 x 50 ms pulses; 25 V
Fig. 7, Fig. S2B-E (miPA2, rescue constructs)	600 ng/µl miRNA construct 350 ng/µl rescue construct	dI1 neuron-specific targeting (*Math1* enhancer-driven) 5 x 50 ms pulses; 25 V

In ovo RNAi with long dsRNA was used where possible, as it is the most efficient method for specific gene silencing. Where required, for example for exclusive targeting of dI1 commissural neurons or for rescue experiments, we used miR constructs.

Supplementary Figures

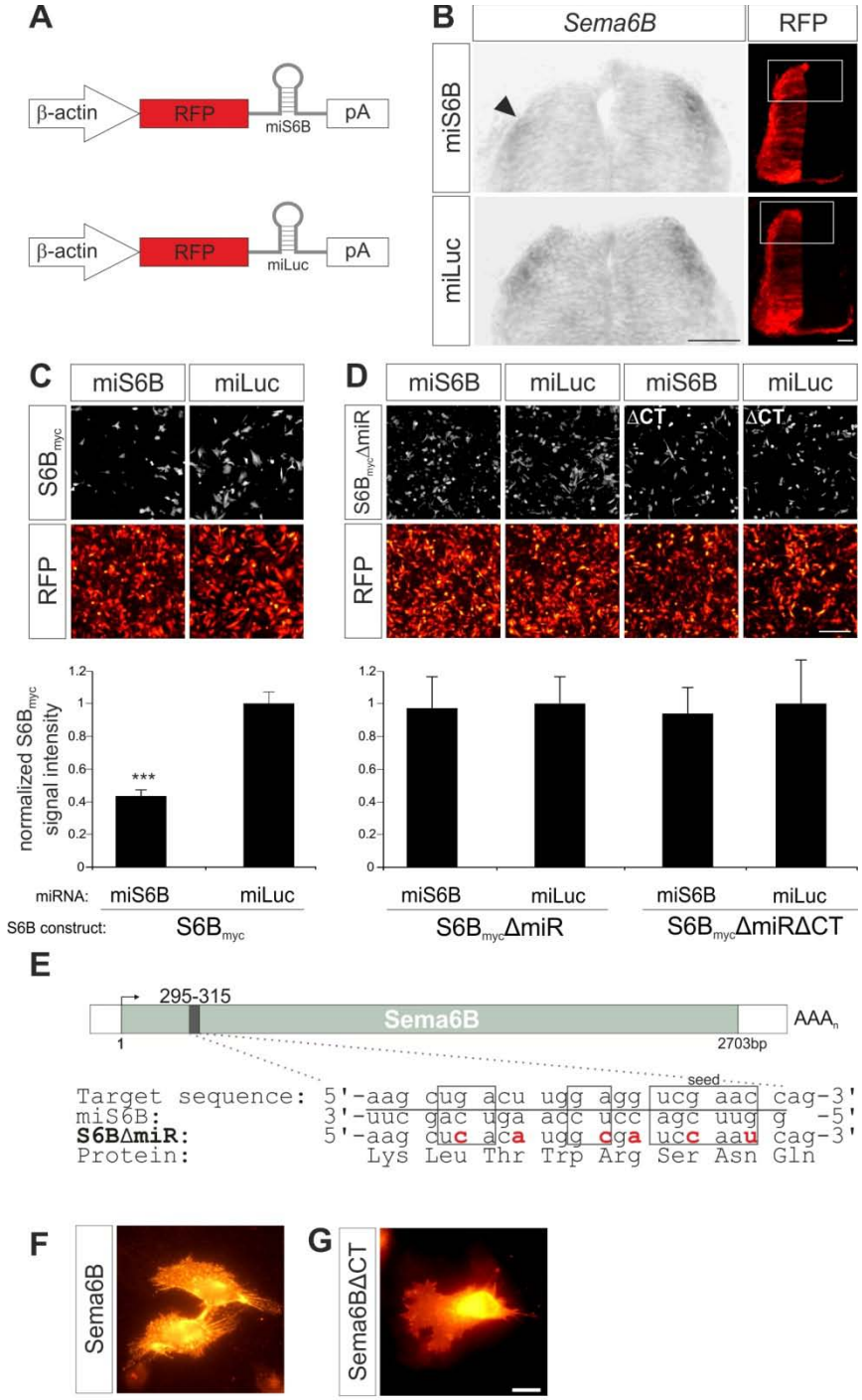

Figure S1

Figure S1. miS6B efficiently downregulates wild-type Sema6B *in vivo* and *in vitro*, but Sema6B containing a mutated miRNA target sequence is resistant to knockdown.

(A) Schematic representations of microRNA constructs against Sema6B (miS6B) and Luciferase (miLuc). (B) *Sema6B* ISH on transverse spinal cord sections taken from embryos expressing miS6B or miLuc. Electroporation of miS6B reduced expression of *Sema6B* on the electroporated side (arrowhead) by 80.5±6.1% (s.e.m.) compared to the control side (n=4 sections from two embryos; $p<0.0005$, t-test). In contrast, electroporation of miLuc did not significantly affect Sema6B expression (staining reduced by 12.4±17.0% (s.e.m.) on the electroporated side compared to the control side; n=5 sections from four embryos; $p=0.253$, t-test). Transfection was visualized by RFP. Scale bar, 50 µm. (C) miS6B efficiently reduced expression of Sema6B in HeLa cells. Myc-tagged Sema6B ($S6B_{myc}$) was reduced by almost 60% when co-transfected with miS6B compared to miLuc. n=28 measurements each; ***$p<0.001$, t-test. (D) miS6B did not reduce the expression of Sema6BΔmiR or Sema6BΔCTΔmiR, two knockdown-resistant forms of Sema6B. The co-transfection of Sema6BΔmiR or Sema6BΔCTΔmiR with either control miLuc or miS6B did not exhibit any significant change in Sema6B/RFP intensity ratios. Ratios were normalized to miLuc control. Scale bars, 100 µm. (E) Design of miRNA-resistant Sema6B for rescue experiments. The region of the Sema6B mRNA that is targeted by miS6B is underlined. Regions important for miRNA target selection and cleavage are indicated by boxes. A miRNA-resistant version of Sema6B (Sema6BΔmiR) was generated by silent mutagenesis of 6 bases in the target region (red). The encoded protein sequence was unaltered. (F) Surface staining of transfected cells revealed that both full-length Sema6B and (G) Sema6BΔCT constructs were efficiently expressed in HEK293 cells and correctly targeted to the membrane (see also Fig.4M). Scale bar, 5 µm.

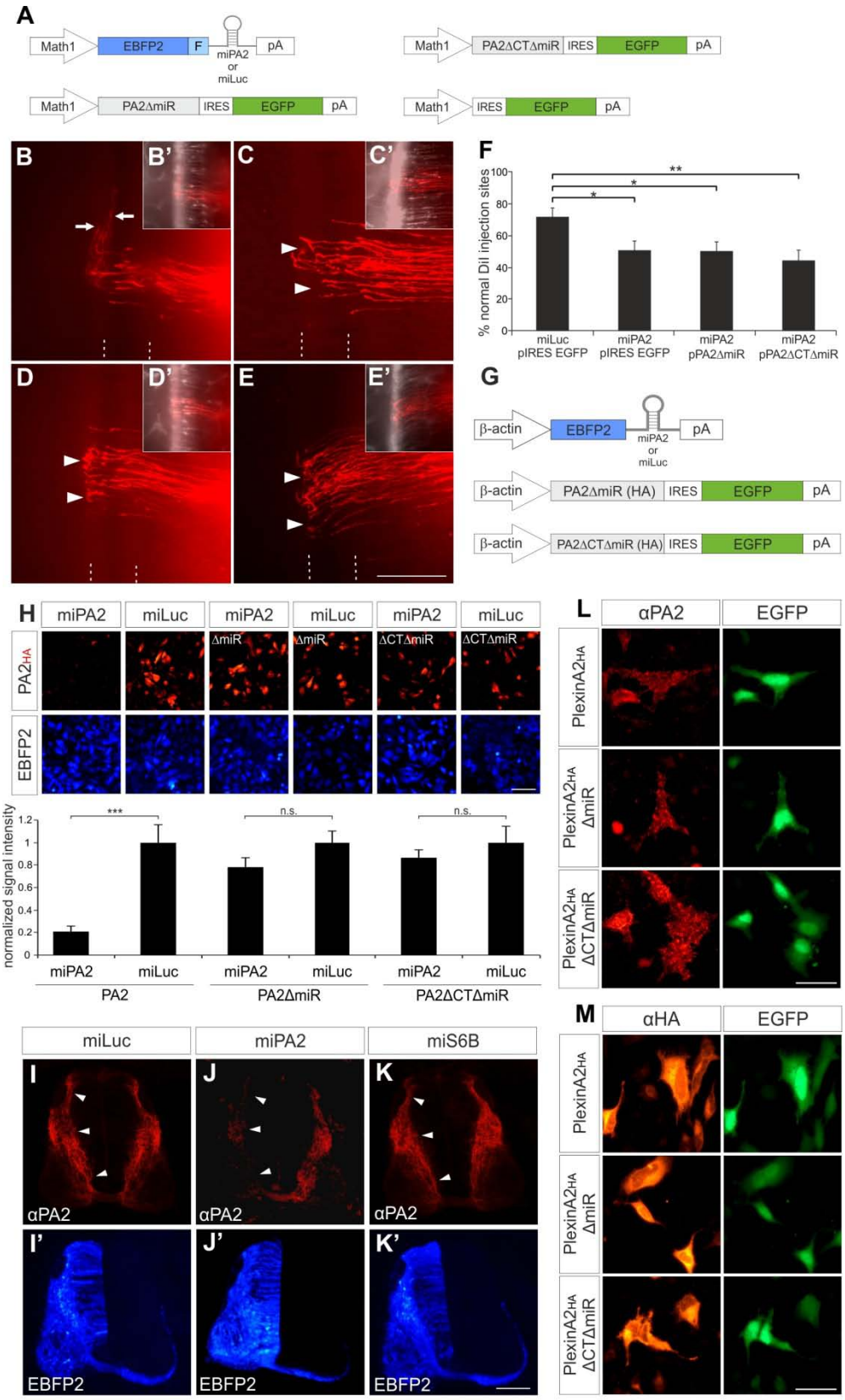
A
Math1
EBFP2
F
miPA2 or miLuc
pA
Math1
PA2ΔCTΔmiR
IRES
EGFP
pA
Math1
PA2ΔmiR
IRES
EGFP
pA
Math1
IRES
EGFP
pA
B
B'
C
C'
D
D'
E
E'
F
% normal DiI injection sites
miLuc pIRES EGFP
miPA2 pIRES EGFP
miPA2 pPA2ΔmiR
miPA2 pPA2ΔCTΔmiR
G
β-actin
EBFP2
miPA2 or miLuc
pA
β-actin
PA2ΔmiR (HA)
IRES
EGFP
pA
β-actin
PA2ΔCTΔmiR (HA)
IRES
EGFP
pA
H
miPA2
miLuc
PA2HA
EBFP2
ΔmiR
ΔCTΔmiR
normalized signal intensity
***
n.s.
PA2
PA2ΔmiR
PA2ΔCTΔmiR
L
αPA2
EGFP
PlexinA2HA
PlexinA2HA ΔmiR
PlexinA2HA ΔCTΔmiR
M
αHA
EGFP
PlexinA2HA
PlexinA2HA ΔmiR
PlexinA2HA ΔCTΔmiR
miLuc
miPA2
miS6B
I
J
K
αPA2
I'
J'
K'
EBFP2

Figure S2

Figure S2. PlexinA2 influences the extension of commissural axons into the ventral spinal cord and their post-crossing turning decision. The PlexinA2 miRNAs and rescue constructs perform as expected.

(A) Schematics of constructs used for dI1 neuron-specific perturbations of PlexinA2. (B) In control embryos co-electroporated with dI1-specific constructs encoding EBFP2-miLuc and the empty *pMath1-IRES-EGFP* plasmid, commissural axons crossed the floorplate and turned rostrally (arrows). (C) Knocking down PlexinA2 with miPA2 resulted in stalling of post-crossing axons at the contralateral floorplate border (arrowheads). The phenotype caused by miPA2 was not rescued by the co-electroporation of PlexinA2ΔmiR (D) or by PlexinA2 lacking the cytoplasmic tail (PlexinA2ΔCTΔmiR) (E; arrowheads). The floorplate is indicated by dashed lines. (B'-E') Merge of DiI-labeled axons (red) and farnesylated EBFP2 (white) used to visualize the expression of different miRNA constructs (EGFP not shown). (F) Quantification of DiI sites with normal axonal pathfinding: control (n=8 embryos, N= 71 injection sites); knock down (n=16, N=137); full-length rescue (n=25, N=228); ΔCT rescue (n=11, N=108). *p<0.05, **p<0.01. (G) Schematic representations of the constructs used in the verification of miPA2 and PA2ΔmiR constructs. (H) HA-tagged PlexinA2 was reduced by almost 80% when co-transfected with miPA2, compared to miLuc (***p<0.001; n=11 and 13 measurements, respectively). However, miPA2 did not reduce the expression of PlexinA2ΔmiR and PlexinA2ΔCTΔmiR, since both constructs contained several silent mutations in the miPA2 target sequence (see Methods). Co-transfection of PlexinA2ΔmiR or PlexinA2ΔCTΔmiR with either control miLuc or miPA2 did not exhibit any significant change in PlexinA2/EBFP2 intensity ratios (12-16 measurements in each condition). Ratios were normalized to miLuc control. Scale bars, 100 µm. (I-K) The downregulation of PlexinA2 upon electroporation of miLuc, miPA2 or miS6B was assessed by PlexinA2 immunoreactivity. In control embryos electroporated with miLuc (I), PlexinA2 expression in pre-crossing commissural axons was no different from the control side. In contrast, PlexinA2 was clearly reduced after electroporation of miPA2 (J, arrowheads). Expression of miS6B (K) did not affect surface levels of PlexinA2 in pre-crossing axons. (I'-K') Successful transfection is visualized by EBFP2 expression. (L-M) Surface and total expression of wildtype and knockdown-resistant PlexinA2 in HEK293 cells. (L) Surface expression was demonstrated by staining HEK293 cells with a PlexinA2 antibody before fixation and permeabilization. Successful transfection was demonstrated by EGFP expression from the same plasmid. (M) For staining total levels of the expressed PlexinA2, cells were fixed and stained with an antibody against the C-terminal HA-tag. Scale bars, 20 µm.

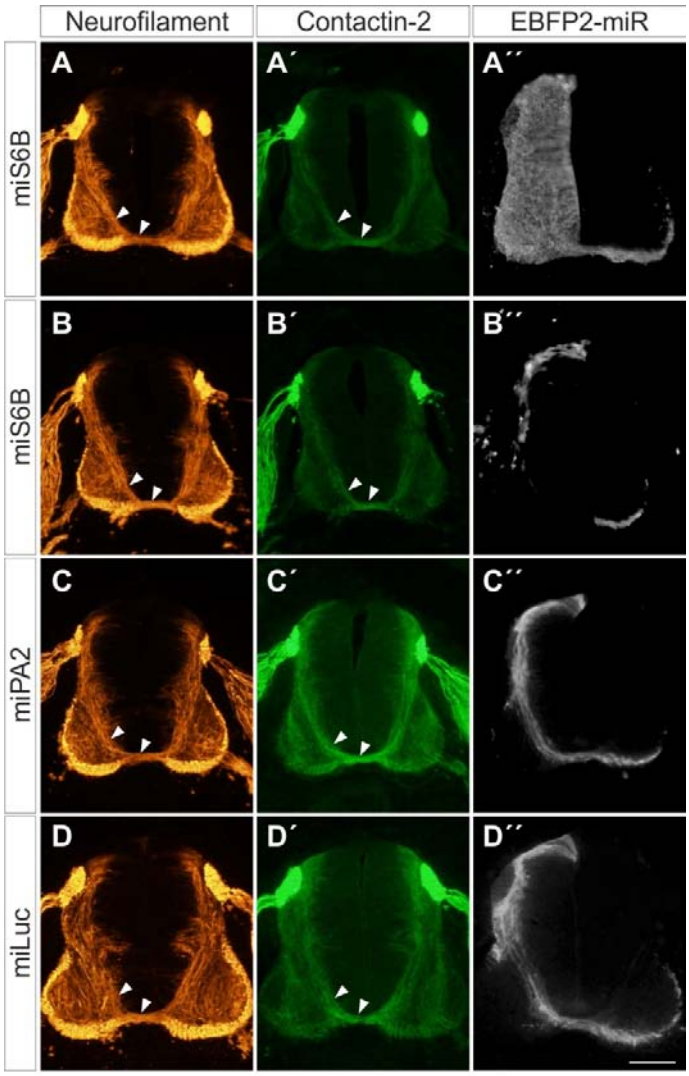

Figure S3

Figure S3. Commissural axon outgrowth is not grossly impaired following the loss of PlexinA2 or Sema6B.

To verify that pre-crossing commissural axon projections were grossly normal following the loss of PlexinA2 or Sema6B, transverse sections of the chicken spinal cord were immunolabeled for neurofilament (A-D) and Axonin1/Contactin2 (A'-D'). Neither unilateral (A-A") nor dorsal (B-B") downregulation of Sema6B impaired the ventral growth of commissural axons compared to controls (D-D"). Similarly, no defects in the ventral projection of commissural axons were observed when PlexinA2 was specifically downregulated in dI1 neurons with Math1-miPA2 (C-C"). Scale bar, 100 µm.

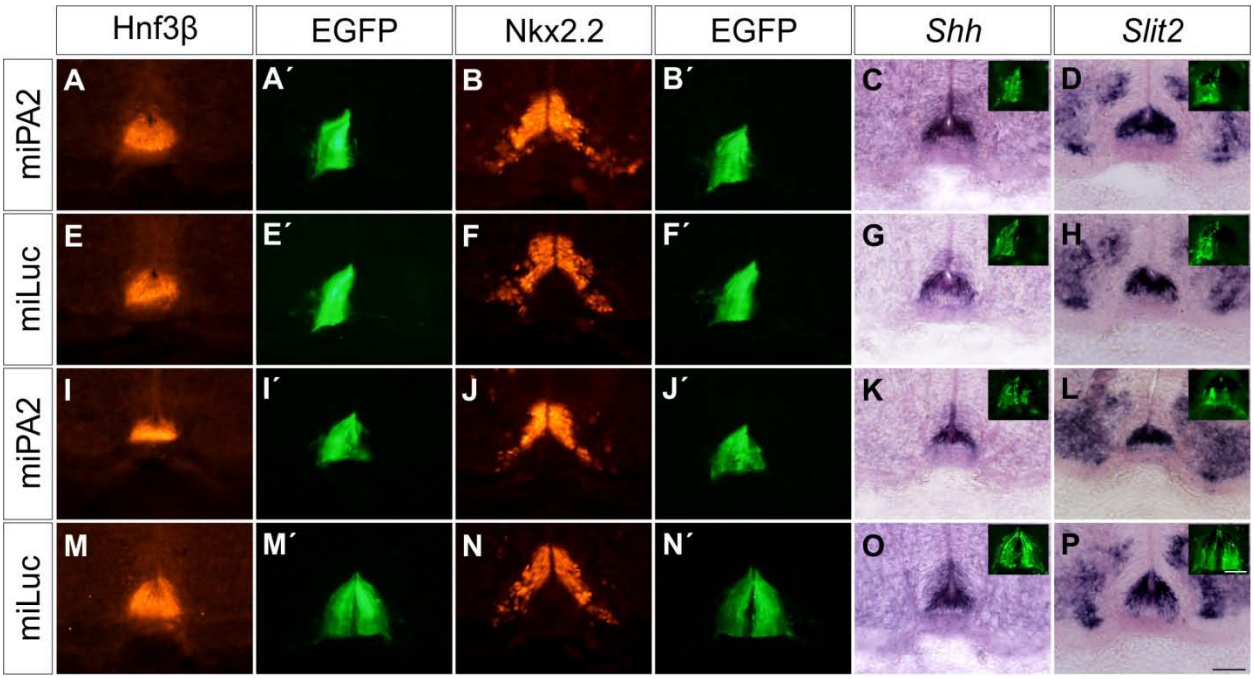

Figure S4

Figure S4. Downregulation of PlexinA2 in the floorplate does not interfere with floorplate morphology or the expression of other axon guidance cues.

To control for a direct effect on commissural axon guidance of PlexinA2 silencing in the floorplate, we analyzed marker expression in the ventral spinal cord after unilateral (A-H) or bilateral (I-P) electroporation of floorplate-specific constructs encoding miPA2 or miLuc. No differences were seen in any condition when we analyzed Hnf3β (A,E,I,M) or Nkx2.2 (B,F,J,N). Similarly, no changes in the expression of *Shh* (C,G,K,O) or *Slit2* (D,H,L,P) were observed. Successful electroporation was verified by GFP expression (A'-N', and insets). Scale bar, 50 µm.

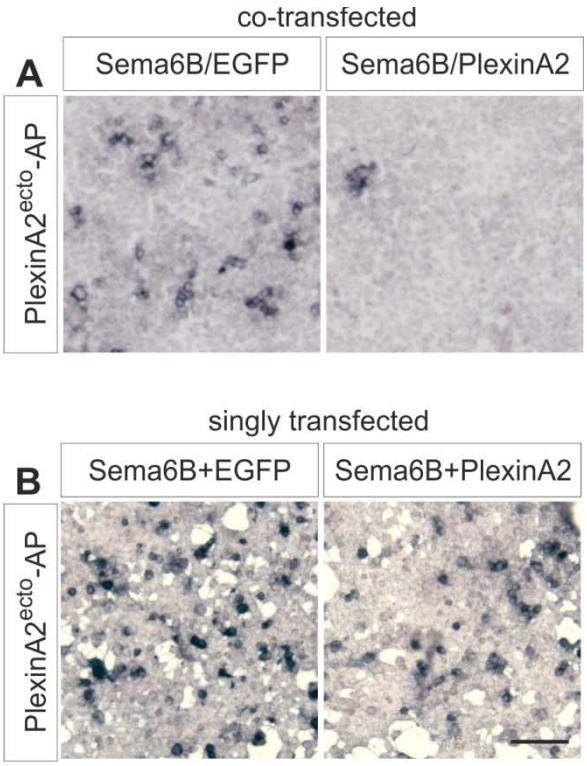

Figure S5

Figure S5. Sema6B/PlexinA2 cis-interaction modulates Sema6B/PlexinA2 trans-interaction.

We assessed the binding of PlexinA2^{ecto}-AP on HEK293 cells transfected with vectors expressing Sema6B and EGFP, or Sema6B and PlexinA2. In panel (A), the cells were co-transfected with the indicated constructs, promoting the formation of cis-complexes. The binding of PlexinA2^{ecto}-AP to Sema6B/PlexinA2 co-transfected cells was markedly reduced compared to binding on Sema6B/EGFP-expressing cells. In panel (B), the cells were separately transfected with Sema6B, EGFP or PlexinA2 and then mixed and replated in the combinations indicated. After single transfections (minimal cis-interactions), the binding of PlexinA2^{ecto}-AP to Sema6B + EGFP cells was comparable to Sema6B + PlexinA2 cells. Scale bar, 100 µm.